Asymmetric Dielectric Trilayer Cantilever Probe for Calorimetric High-Frequency Field Imaging

Simone Lee, T. Mitch Wallis, John Moreland, Pavel Kabos, *Fellow, IEEE*, and Y. C. Lee, *Fellow, ASME*

***Abstract*—Multimaterial, microelectromechanical systems-based cantilever probes were developed for high-frequency magnetic field imaging. The basic configuration of the probe consists of a cantilever beam fabricated using surface micromachining and bulk micromachining techniques with dielectric silicon nitride and silicon oxide materials on a silicon wafer. A gold patterned metallization at the tip of the cantilever provides a source of eddy current heating due to the perpendicular component of the high-frequency magnetic field. This thermally absorbed power is converted to mechanical deflection by a multimaterial trilayer cantilever system. The deflection is measured with a beam-bounce optical technique employed in atomic force microscopy systems. We discuss the modeling, design, fabrication, and characterization of these field imaging probes. [1727]**

***Index Terms*—Curvature, high-frequency imaging, microelectromechanical systems (MEMS) cantilever, radio-frequency (RF) probe.**

I. Introduction

With the rapid development of high-speed electronics, the density of on-chip components and the frequency of operating signals have recently increased dramatically. As a result, there is a need to measure the electromagnetic interference between different parts of the circuit and/or coupling of on-chip components. Existing magnetic field measurement probes use a wire loop to measure the induced voltage or current across the wire loop [1], [2]. The spatial resolution of these systems is limited by the magnetic flux passing through the loop and is thus limited by the area of the loop. The spatial resolution is typically on the order of 1 mm to tens of micrometers [1], [2]. Furthermore, the radio frequency (RF) that the system can measure is limited by the resistance and inductance (RL) time constant of the wire and is typically in the megahertz or low-gigahertz range. This paper discusses the development of a new type of probe to serve as a near-field high-spatial resolution and broadband sensor to measure the perpendicular component of microwave magnetic field.

Manuscript received November 25, 2005; revised April 11, 2006. Subject Editor H. Zappe.

S. Lee was with the University of Colorado at Boulder, CO 80309 USA. She is now with FormFactor Inc., Livermore, CA 94551 USA (e-mail: SLee2@FormFactor.com).

T. M. Wallis, J. Moreland, and P. Kabos are with the National Institute of Standards and Technology, Boulder, CO 80305 USA (e-mail: kabos@boulder.nist.gov).

Y. C. Lee is with the Department of Mechanical Engineering, University of Colorado at Boulder, CO 80309 USA (e-mail: leeyc@colorado.edu).

Color versions of one or more of the figures in this paper are available online at http://ieeexplore.ieee.org.

Digital Object Identifier 10.1109/JMEMS.2006.885849

Jander *et al.* [4] demonstrated calorimetric magnetic field measurement probes based on microelectromechanical systems (MEMS) structures. The magnetic field detection discussed in [4] is based on heating of the probe via the ferromagnetic resonance induced in the material positioned at the tip of the probe. An external magnetic field bias is required. The limit of such a configuration is that the sensor can be used only at the resonant frequency of the ferromagnetic material. Our device avoids the use of ferromagnetic materials and uses instead eddy current heating of nonmagnetic materials. We will discuss this in the next section.

Calorimetric probes using bimorph cantilevers have been used as femtojoule calorimeters in [5]. A commercial silicon nitride atomic force microscope (AFM) probe is coated with aluminum on one side of the cantilever to create a bimorph structure. The deflection of the cantilever is measured as a function of power absorbed by the aluminum layer. Similar calorimetric sensors for microwave absorption measurements have been described in [6], where magnetic materials were deposited onto commercial silicon AFM cantilevers. Bimorph cantilever structures of 2-μK sensitivity were also used as temperature sensors in [7]. The bimorph system is optimized by tuning the thickness ratio of the aluminum and silicon nitride system.

The objective of this paper is to design and fabricate a multimaterial probe for sensing the magnetic field component by use of a calorimetric approach. To decrease the eddy current contribution, the cantilever structure has to be made of dielectric materials, as will be discussed below. However, the fabrication of dielectric bimorph cantilevers creates curling problems, thus rendering them unusable for measurements. For optical geometry of our homemade scanning probe measurement system, the cantilever must have a tip deflection of less than 50 μm or a radius of curvature of more than 2.5 mm. This specification can be achieved by utilizing an asymmetrical trilayer design. Specifically, the cantilever structure is made of nitride–oxide–nitride, with different thicknesses for the top and bottom nitride layers. In Section III, we discuss an analytical model of a bimorph and trilayered cantilever and compare the model with finite-element analysis (FEA). The fabrication process and experimental results will be discussed in Sections IV and V, respectively. The MEMS probe will be used as a sensor that converts thermal power absorbed from the high-frequency magnetic field component to mechanical deflection.

II. Sensing Mechanism

A MEMS-based probe was designed and fabricated to detect the magnetic field component radiated by an RF circuit. The

1057-7157/$25.00 © 2007 IEEE

Authorized licensed use limited to: IEEE Xplore. Downloaded on November 24, 2008 at 14:41 from IEEE Xplore. Restrictions apply.

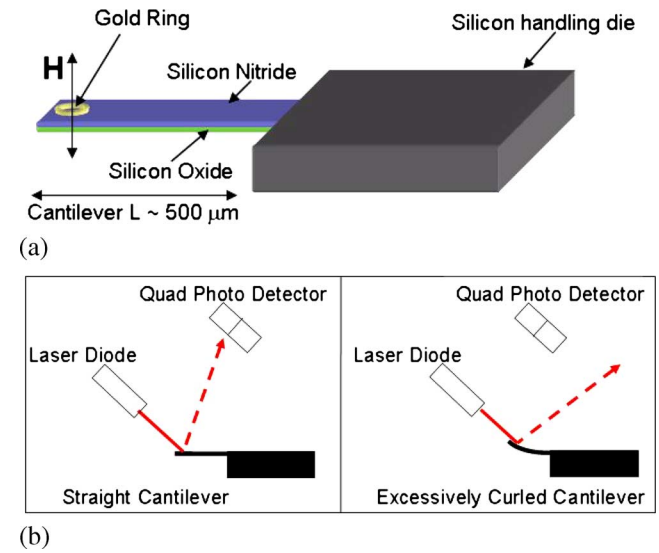

Fig. 1. Schematics of (a) the basic configuration of the MEMS probe and (b) misalignment problem due the curled cantilever.

TABLE I
MATERIAL PROPERTIES OF SILICON NITRIDE AND LOW-TEMPERATURE OXIDE [8]

	SiNx	LTO
Young's Modulus [GPa]	300	70
CTE [ppm/°C]	3.2	0.5
Poisson's ratio	0.22	0.17

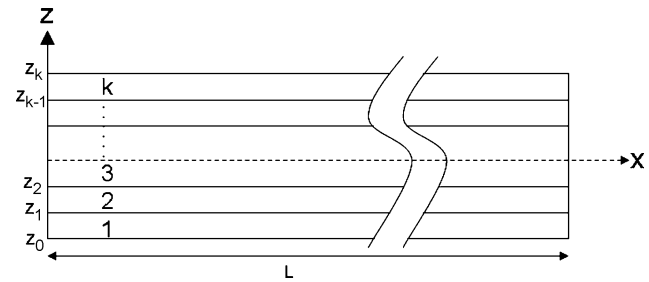

Fig. 2. Multilayer film system coordinates convention.

basic configuration of the probe consists of a cantilever beam fabricated from silicon nitride and silicon oxide on a silicon wafer [see Fig. 1(a)]. A gold ring is patterned at the tip of the cantilever as an actuation/detection sensor. A metal of higher resistivity could be used to achieve a greater heating effect [6]. However, gold was chosen for the ease of deposition and patterning purposes. Fig. 1(a) shows the basic configuration of the bimorph cantilever probe. A time-varying magnetic flux from the RF circuit passing through the gold ring induces an electromotive force, according to Faraday's law. Induced current is linearly proportional to the magnitude of the magnetic field. This current generates joule heating in the gold ring, resulting in a temperature gradient across the body of the cantilever. The cantilever deflects due to the different coefficients of thermal expansion of the two dielectric materials. Tip deflection is measured with the laser beam bounce technique routinely employed in AFM systems. A laser beam is focused onto the tip of the cantilever, and is reflected back to a quad-photodiode detector. The change in the photodiode differential signal is a proportional measure of the deflection of the cantilever.

III. PROBE MODELING

To understand the behavior of the multimaterial cantilever under the thermally induced stress, we modeled its deflection as a function of current magnitude for different layer configurations using a commercially available FEA package. The material properties of the multimaterial cantilever are listed in Table I. The dielectric films were deposited by low-pressure chemical vapor deposition (LPCVD) in a furnace at elevated temperature. The differences in the deposition temperature for the different layers of the cantilever lead to a thermal misfit strain and residual stresses between the layers. Due to this stress, the cantilever will naturally curl. This curling of the cantilever is undesirable for the optical beam-bounce technique. Misalignment of the laser with the detector will occur when the curling of the cantilever is too large, due to the limited adjustment and degrees of freedom of the optics in the AFM-like system. This misalignment is illustrated in Fig. 1(b).

We modeled the fabrication-induced curling of the cantilever by Kirchhoff's plate theory for multilayer thin films [9]–[11]. First, a bimorph model is discussed. The analytical predictions are compared with FEA simulations for the shape of the cantilever in the curling state. To reduce the curvature of the cantilever, an asymmetric trilayer model is introduced, and an example is discussed in order to illustrate the design of a probe that will meet the required specifications.

A. Bimorph Model

The basic configuration of the cantilever probe consists of a bimorph cantilever similar to the device described in [4]. The cantilever probe in [4] was fabricated with 500-nm silicon nitride and 500-nm silicon oxide layer thicknesses. The length and width of the cantilever in [4] were $L = 500$ and $w = 50\ \mu$m, respectively. We used Kirchhoff's plate theory for multilayer film systems [9]–[11] to estimate the cantilever curvature. The mid-plane strain (ε_o) and curvature (κ) of the system can be written in this form [10]

$$\begin{bmatrix} \varepsilon_o \\ \kappa \end{bmatrix} = \begin{bmatrix} A & B \\ B & D \end{bmatrix}^{-1} \left[\begin{Bmatrix} N_\varepsilon \\ M_\varepsilon \end{Bmatrix} - \begin{Bmatrix} N_\sigma \\ M_\sigma \end{Bmatrix} \right] \tag{1}$$

where $A = \sum_{k=1}^{n} w_k Q_k (z_k - z_{k-1})$ is the extension stiffness, $B = (1/2) \sum_{k=1}^{n} w_k Q_k (z_k^2 - z_{k-1}^2)$ is the coupling stiffness, $D = (1/3) \sum_{k=1}^{n} w_k Q_k (z_k^3 - z_{k-1}^3)$ is the bending stiffness, $Q_k = E_k/(1 - \nu_k)$ is the biaxial modulus, E is the Young's modulus, ν is the Poisson's ratio of materials, and w is the width of the plate. The subscript k represents the index of the kth layer of the multilayer film system (Fig. 2). The term z_k refers to the interface of the laminates of the kth layer with respect to the mid-plane of the system. The resultant force per unit length (N) and the resultant moment per unit length (M) contain two influential contribution terms. The first contribution (N_ε and M_ε comes from the thermal misfit strain in the multilayer structure due to the temperature changes during the film deposition processes discussed above. The second contribution (N_σ and M_σ)

Authorized licensed use limited to: IEEE Xplore. Downloaded on November 24, 2008 at 14:41 from IEEE Xplore. Restrictions apply.

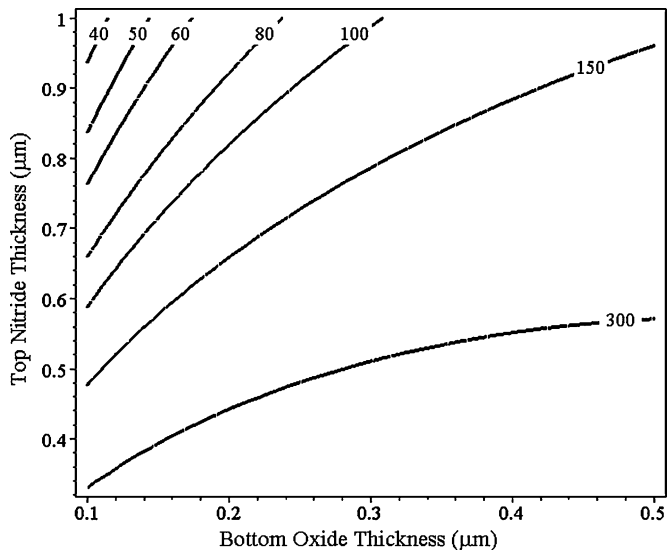

Fig. 3. Analytical solution of a bimorph cantilever tip deflection (in micrometers) due to thermal misfit strain as a function of the thickness of nitride and oxide.

is the initial intrinsic residual stress within the thin films itself formed during deposition. The resultant force and moment per unit length that result from thermal misfit strain, are defined as

$$N_\varepsilon = \sum_{k=1}^{n} w_k Q_k (z_k - z_{k-1}) \mathrm{CTE}_k (T_r - T_k)$$
$$M_\varepsilon = \frac{1}{2} \sum_{k=1}^{n} w_k Q_k \left(z_k^2 - z_{k-1}^2\right) \mathrm{CTE}_k (T_r - T_k) \qquad (2)$$

where CTE is the coefficient of thermal expansion and T_r and T_k are the room and stress-free temperatures, respectively. The resultant force and moment per unit length resulting from the intrinsic residual stress due to deposition are defined as

$$N_\sigma = \sum_{k=1}^{n} w_k \sigma_k (z_k - z_{k-1})$$
$$M_\sigma = \sum_{k=1}^{n} w_k \left\{ \frac{\sigma_k}{2} \left(z_k^2 - z_{k-1}^2\right) - \frac{\beta_k}{12} (z_k - z_{k-1})^3 \right\} \qquad (3)$$

where σ is the average intrinsic residual stress measured with wafer curvature method and β is the stress gradient through the thickness of the film ($\beta = \kappa \mathrm{E}$ for a single layer cantilever; its value is small and can be ignored in this paper).

The curvature of the multilayer systems can then be obtained from (1)

$$\kappa = \frac{-B \cdot (N_\varepsilon - N_\sigma) + A \cdot (M_\varepsilon - M_\sigma)}{A \cdot D - B^2}. \qquad (4)$$

For this analysis, we assume that the thermal mismatch strain is the only source of inelastic strain in the system. Further, we assume that the tip deflection δ relates to the curvature by $\delta = \kappa \mathrm{L}^2/2$. Fig. 3 shows plots of different tip deflections (contour lines) of a bimorph cantilever as a function of the nitride and oxide thicknesses ranging from 100 (minimum deposited thickness) to 500 nm, from (4). For laser alignment purposes, the tip deflection should be less than 50 μm for the geometry of our optical measurement system. This plot shows that this requirement cannot be achieved with a bimorph system.

This undesirable curling of the cantilever is more difficult to eliminate in this system than in other bimorph devices. Stress due to fabrication in other devices can be removed by annealing at elevated temperature if the materials are polycrystalline, e.g., polysilicon. The grain growth during annealing can relieve stress in thin crystalline films [11]. However, the materials used in this paper are amorphous dielectric materials. Stress in these kinds of materials cannot be removed by using conventional methods (such as annealing). A multilayered structure can reduce the curvature.

B. Asymmetric Trilayer Model

The initial curvature of the cantilever associated with fabrication-induced stress can be minimized by use of a trilayered nitride–oxide–nitride structure. When the thicknesses of the top and bottom nitride layers are exactly the same, the cantilever will not bend with temperature change, since expansion of the top layer balances with the expansion of the bottom layer, regardless of the expansion of the middle layer. If the thicknesses of the top and bottom nitride layers differ slightly, the cantilever is less likely to curl due to fabrication temperature change but is sensitive to temperature gradients induced by eddy current heating. In Fig. 4(a), the initial tip deflection δ (in micrometers) of the cantilever is plotted as a function of the top layer nitride thickness (abbreviated as N2) and middle layer oxide thickness (abbreviated as LTO) when the bottom layer nitride thickness (abbreviated as N1) is fixed at 100 nm. Fig. 4 shows that the curvature is not a strong function of oxide thickness; instead, it depends strongly on the top layer nitride thickness. For a fixed oxide thickness of 500 nm, the tip deflection is plotted as a function of the bottom and top nitride thicknesses Fig. 4(b). For a tip deflection below 50 μm (curling upwards with respect to the silicon handling die), a design that achieves our target curling is a top nitride thickness of 190 nm and a bottom nitride thickness of 150 nm. We can see in Fig. 4 that other combinations of top and bottom nitride thicknesses within the contour lines $\delta = 0$ to $\delta = 50$ are possible choices.

C. Finite Element Modeling

In addition to the analytical model, we implemented finite-element modeling (FEM) to analyze the fabrication-induced curling of the bimorph and trilayer cantilevers. The mechanical boundary condition for the MEMS probe is fixed at one end of the cantilever. The stress-free temperature for each material is set at the deposition temperature of 835 °C for silicon nitride and 450 °C for silicon oxide. The model is then relaxed to room temperature (20 °C) to obtain the initial deformation due to the thermal misfit strain during fabrication. Fig. 5 shows a typical simulation result for the initial curling of the cantilever. For a bimorph cantilever length of 500 μm and width of 25 μm and with 500-nm-thick silicon oxide and 500-nm-thick silicon nitride thicknesses, the tip deflection from thermal mismatch strain is about 310 μm. These simulation results are in good

Authorized licensed use limited to: IEEE Xplore. Downloaded on November 24, 2008 at 14:41 from IEEE Xplore. Restrictions apply.

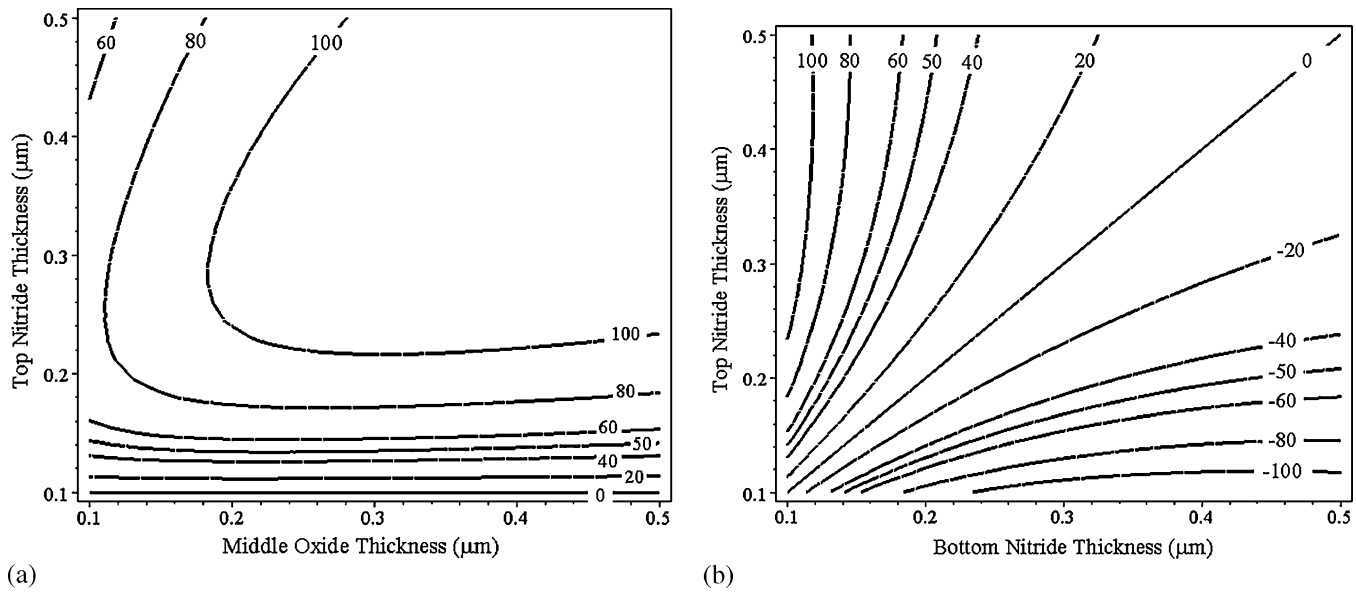

Fig. 4. Analytical solution of an asymmetric trilayer (NON) cantilever tip deflection: (a) bottom nitride thickness fixed ($N1 = 100$ nm) and (b) middle oxide thickness fixed LTO ($= 500$ nm).

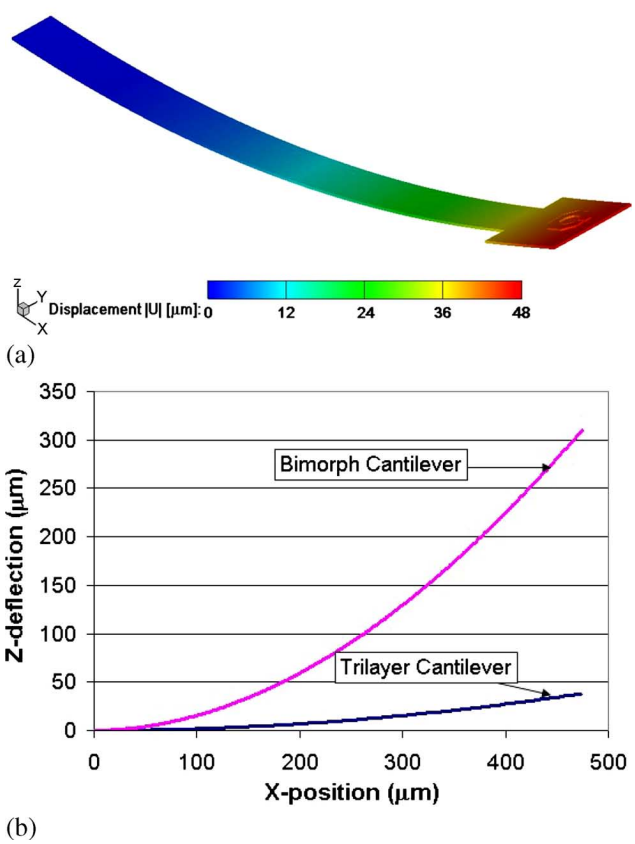

Fig. 5. (a) FEM simulation result for the thermal misfit strain created during fabrication, cantilever with thicknesses of $N1 = 150$ nm, LTO $= 500$ nm, and $N2 = 200$ nm are used in the simulation. (b) FEM result of the initial curling of a bimorph cantilever (with nitride and oxide thicknesses of 500 nm, respectively) and a trilayer cantilever along its length.

agreement with the analytical solution of (4). Fig. 5 compares the FEM results for the bilayer and the trilayer cantilevers. A significant reduction of curvature is achieved with trilayer structures. Fig. 6 shows the deflection along the cantilever length obtained with an interferometer measurement and can be seen the model and the fabricated cantilevers are in good agreement. Thus, this trilayer structure can also be used in other MEMS devices requiring a precise control of the curvature of the structure. The curvature of the cantilever can be tuned by varying the thickness ratio of the top to bottom nitride layers.

D. Sensitivity to Eddy Current Heating

The deflection of the cantilever from eddy current heating is obtained by finite-element simulation. We assume that the eddy current power absorption can be represented by joule heating of the gold ring. In the modeling, a current is applied to the gold ring to obtain a temperature distribution and deflection of the cantilever. The boundary conditions are as follows: the end of the cantilever is fixed in the x, y, and z directions, with the temperature at the same end of the cantilever set at room temperature (the end is attached to the silicon handling die, which acts as a heat sink). Joule heating $P = I^2 R$ (where R is the resistance) creates a temperature distribution across the cantilever. The temperature gradient changes the curvature or tip deflection of the cantilever because of the different thermal expansion of the nitride and oxide layers. The change between the initial state and the deflection caused by the applied current gives the deflection as a function of the applied current.

Due to fabrication variations, the thicknesses of the cantilevers may differ by $+/-10\%$ depending on the location of the cantilever within the wafer and the position of the wafer relative to the furnace during deposition. To include this possibility, the simulation is repeated with the thickness of the three layers varying from -10% to $+10\%$ with respect to the average thicknesses in each layer. Fig. 7 shows the resulting deflection of different cantilevers as a function of eddy current heating. From the simulation, we conclude that the sensitivity

Authorized licensed use limited to: IEEE Xplore. Downloaded on November 24, 2008 at 14:41 from IEEE Xplore. Restrictions apply.

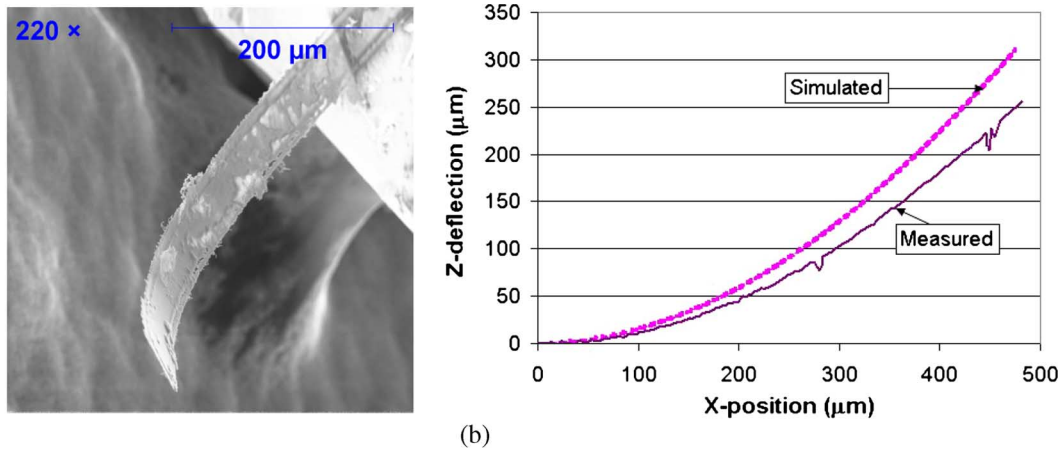

Fig. 6. (a) SEM photograph of a fabricated bimorph cantilever. (b) Graph showing the measured initial curling of the bimorph cantilever along the length and FEA model result.

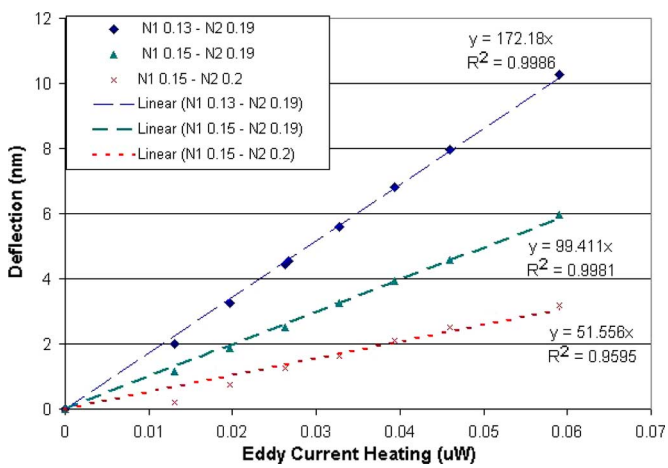

Fig. 7. FEA simulation results showing the deflection as a function of eddy current heating for three cantilevers.

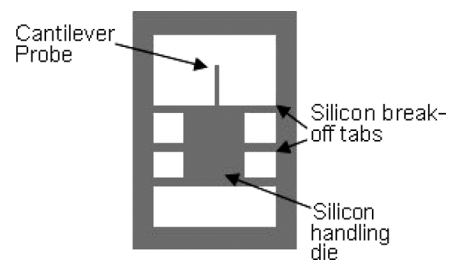

Fig. 8. Schematic of the mask for the cantilever structure, silicon breakoff tabs, and silicon handing die (diagram not drawn to scale).

TABLE II
LPCVD DEPOSITION PARAMETERS

	SiN_x	LTO
Deposition Rate (Å/min)	50	200
Chemical Flow Rate (sccm)	NH_3 - 12 $SiCl_2H_2$ - 59	O_2 - 65 SiH_4 - 100
Temperature (°C)	835	450
Deposition Pressure (mTorr)	250	300

of the probe is very susceptible to the change in thickness of the nitride layers.

IV. FABRICATION OF THE PROBE

A. Initial Fabrication Method

Following the results of the analytical and numerical simulation, the cantilever probe was fabricated on a double-side polished ⟨100⟩ silicon wafer. The wafer was cleaned with buffered oxide etch (BOE) to strip off the native oxide before deposition. The step-by-step process flow of the cantilever is shown in Fig. 9(a). A 300-nm layer of silicon nitride (SiNx) was deposited with LPCVD, and then a 500-nm layer of low-temperature silicon oxide (LTO) was subsequently deposited on the first silicon nitride layer (steps 1 and 2 in Fig. 8). A 300-nm layer of SiNx was used to account for etching from the final etching step 9 in Fig. 8(a) in order to obtain a 100-nm bottom nitride thickness. Table II shows the processing parameters for the two depositions. These two layers were patterned into the cantilever geometry by use of reactive ion etching (RIE) on the front side of the wafer [step 3 in Fig. 8(a)]. The etch recipe is shown in Table III, and the etch mask used for this cantilever geometry is shown in Fig. 8. In step 4, a second layer of SiNx was deposited onto the patterned layers to serve as a protection of the middle oxide layer during subsequent etching steps and the bottom layer of the cantilever. In step 5, a gold ring was deposited by e-beam evaporation and patterned at the end of the cantilever by use of a liftoff technique. From the backside of the wafer, the stacked nitride-oxide-nitride layers were patterned to create openings for additional silicon wet etching. The silicon wafer was then etched from the backside by deep RIE (DRIE) for two-thirds of the thickness of the wafer. For DRIE, the standard Bosch process is used, where a mixture of SF_6 and O_2 is used for etching, and C_4F_8 is used for passivation. A mixture of 30% wt KOH and 2% vol. isopropyl alcohol (IPA) was used to wet-etch silicon at 75 °C. The back-side silicon was etched until the front-side nitride layer was reached. The cantilevers were released from the wafer by removing the nitride membrane from the backside with plasma etching.

The fabrication process described relies on the second nitride layer to serve as the protection of the oxide layer and as the membrane to support the cantilever before release (but after KOH removal of the silicon under the cantilevers). During the release of the cantilever, plasma etching was used to remove

Authorized licensed use limited to: IEEE Xplore. Downloaded on November 24, 2008 at 14:41 from IEEE Xplore. Restrictions apply.

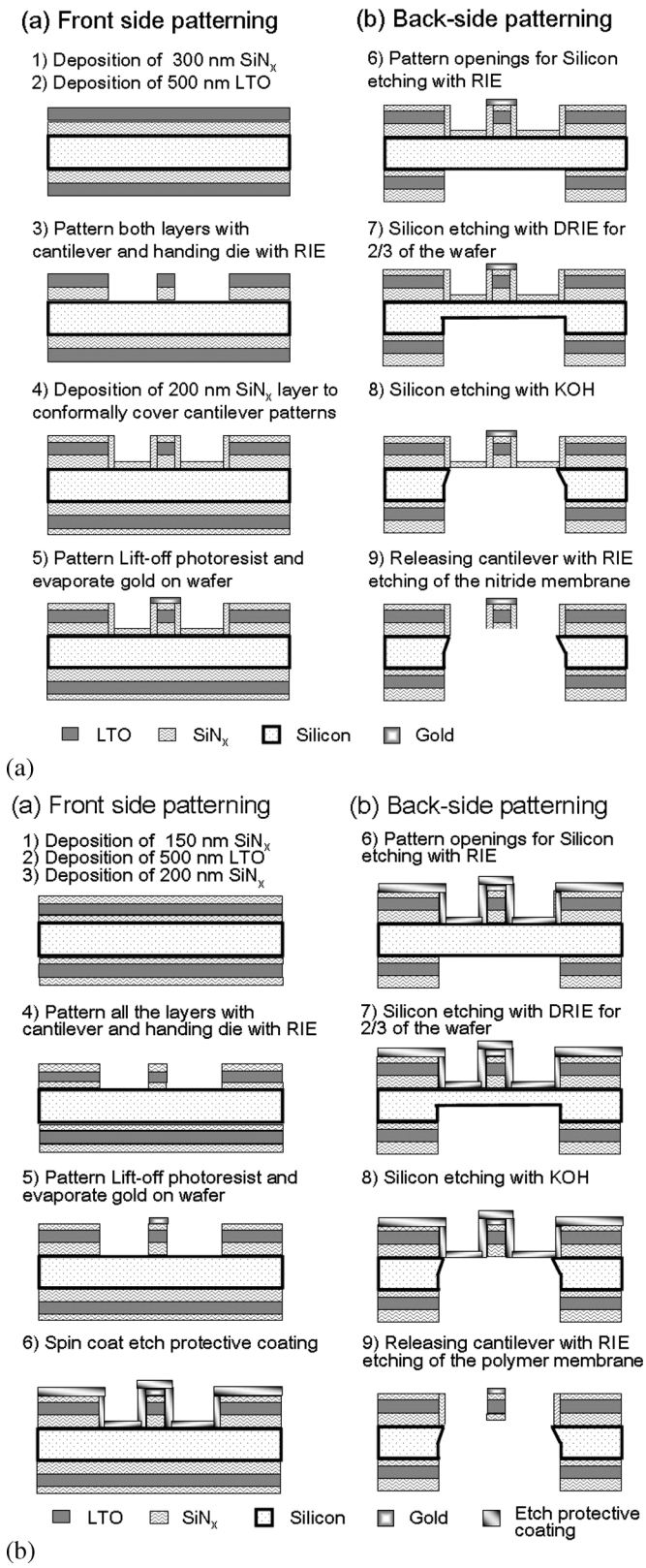

Fig. 9. Fabrication process flow: (a) method 1 and (b) enhanced method (diagram not drawn to scale).

the nitride membrane from the back side of the wafer to avoid damage to the cantilevers by contact with liquid chemicals. The plasma release was performed with the wafer facing down onto a clean silicon wafer; thus the nitride membrane was removed from the back side. The etch time was controlled so that a thin layer of nitride remained on the bottom of the cantilevers.

This method successfully fabricates working devices. However, the resulting thickness of the bottom nitride layer is not consistent across the wafer. Consequently, the initial curling of the cantilever is not uniform across the wafer, leading to low yield. Defective cantilevers are those with curvature too high for laser alignment to be possible during measurement.

TABLE III
ETCHING RECIPE FOR SiNx, LTO, AND ETCH-PROTECTIVE COATING

	Etching SiN_x or LTO	Etching etch-protective coating
Chemicals Flow (sccm)	CF_4 - 42 O_2 - 2	O_2 - 50
Process Pressure (mTorr)	35	150
RF Power (W)	150	100
Etch rate (nm/min)	~ 35 for SiN_x ~ 25 for LTO	~ 20

B. Enhanced Fabrication Method

To improve the process yield, the fabrication method was slightly modified; the process flow diagram is shown in Fig. 9(b). The process starts with a ⟨100⟩ double-sided polished silicon wafer cleaned in BOE. A 100-nm LPCVD SiNx was deposited onto the wafer, followed by deposition of 500-nm LTO and 200-nm LPCVD SiNx, respectively. The nitride–oxide–nitride (N–O–N) stacked layers were then patterned with the cantilever structure by use of the RIE. Gold rings were patterned by use of the liftoff technique. An etch-protective layer [13][1] was coated on the front side of the wafer. From the back side of the wafer, openings were patterned with RIE for silicon etching. DRIE was used to etch the silicon wafer for two-thirds of the thickness. The remaining silicon wafer was etched with 30% wt. KOH (with 2% IPA) at 75 °C until the top etch-protective layer was reached. The cantilever probes can be released by etching the etch-protective layer in O_2 plasma. The etching parameters are summarized in Table III.

The key feature of this improved process is the use of an etch-protective layer to coat the front side of the wafer. The layer serves as a membrane to support the cantilevers before release of the probes and provides protection of the wafer while immersed in the KOH solution. The cantilevers were released by an O_2 plasma etch of the protective layer or an acetone and isopropanol dip. This releasing method has the selectivity of removing only the etch-protective layer without damaging the nitride and oxide layers, whereas, in the previous method, the plasma etch release recipe etches both the nitride and the oxide layers, which leads to poor thickness control of the cantilevers.

The fabricated cantilever is shown in Fig. 10. Three designs of the cantilever were fabricated. Table IV lists the design thickness and the average measured thicknesses (+/−10%) for the

[1]Available from Brewer Science. Trade name is provided for technical clarity and does not imply endorsement by NIST. Products from other manufacturers may perform as well or better.

Authorized licensed use limited to: IEEE Xplore. Downloaded on November 24, 2008 at 14:41 from IEEE Xplore. Restrictions apply.

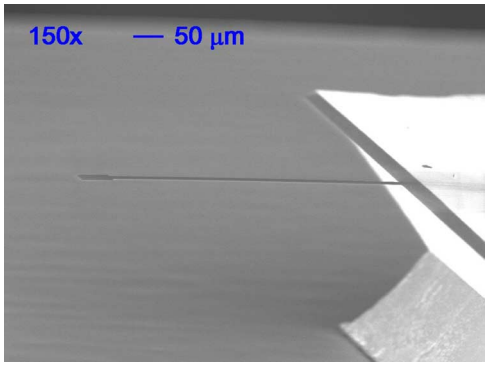

Fig. 10. SEM photograph of a fabricated trilayer cantilever probe.

TABLE IV
CANTILEVER DESIGN PARAMETERS

Design	A	B	C
Designed thickness N1, LTO, N2 [nm]	150, 500, 190	120, 500, 150	100, 400, 366
Average measured thickness [nm]	140, 490, 210	115, 510, 170	100, 370, 280
Simulated tip deflection due to thermal misfit strain [μm]	39-45	45-55	100-120
Average measured tip deflection [μm]	8 +/- 1	100 +/- 5	110 +/- 10

three layers, simulated tip deflection due to thermal misfit strain, and measured tip deflection average of five cantilevers across the 3-in wafer. The variation of the initial tip deflection of the cantilever across the wafer is due to the variation of the thicknesses of the three layers during the low pressure chemical vapor deposition. Note that the measured thicknesses of the layers are typically within 10% of the design due to the control limitation of the deposition thickness.

The difference in the measured tip deflection of the fabricated cantilever and the simulated deflection is due to the simulation's having included only the thermal misfit strain of the three layers. Residual stresses could also develop during the thin-film deposition [13], [14]. These residual stresses cause a change in the final curvature of the cantilever.

V. POWER MEASUREMENT

The experiment was conducted with the asymmetrical trilayer cantilever positioned above a microstrip resonator; see Fig. 1(c). Optical detection of the cantilever deflection is similar to a commercial AFM system. Fig. 11 shows a photograph of the experimental setup. The cantilever probe was positioned at about 100 to 300 μm above the center of the microstrip resonator. The resonant frequency is designed at 9.55 GHz. The microwave output from the sweeper was amplitude modulated by an 11-Hz sine wave. The depth of modulation is chosen such that it turns the RF power on and off at 11 Hz. The sine wave also serves as a reference signal for the lock-in amplifier to measure the difference in the output of the photodetector. We paired segments of the quad photodetector to effectively split the detector into just two halves. The difference in the intensity at the top and the bottom half of the detector yields the deflection of the cantilever probe. The deflection of the cantilever probe was measured as a function of applied RF power to the microstrip line.

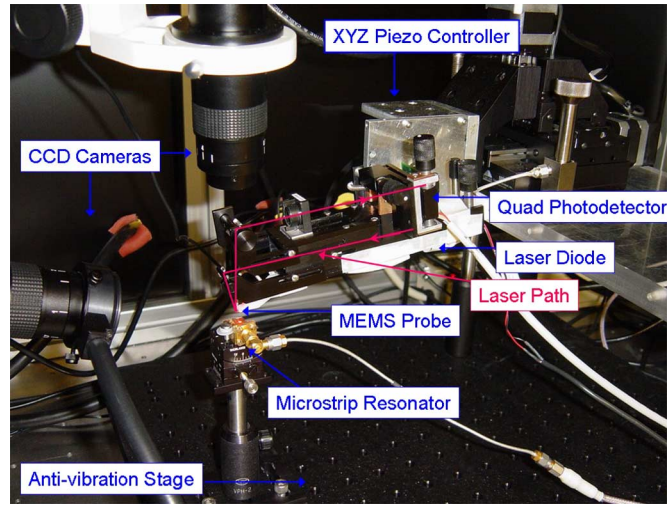

Fig. 11. Photograph of the experimental setup showing the scanning head and the RF circuit microstrip resonator.

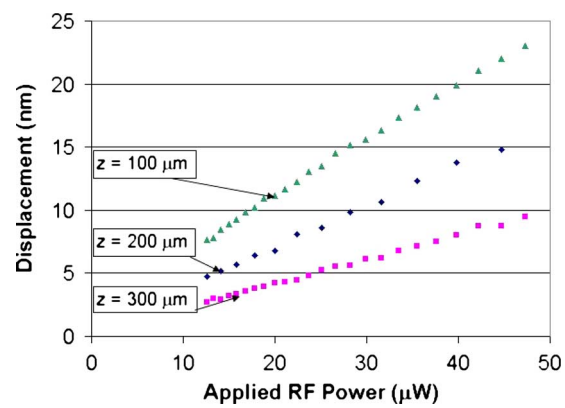

Fig. 12. Measurement results showing the deflection of the cantilever as a function of applied RF power at three locations.

Experiments were performed to verify the field sensitivity of the probe. The power dependence of the cantilever was measured at three locations: 100, 200, and 300 μm above the edge of the microstrip resonator. Fig. 1(c) shows a schematic of the MEMS probe and the microstrip resonator. A plot of measured deflection (nm) as a function of applied RF power (mW) is shown in Fig. 12. The graph shows that the deflection is linearly proportional to the applied RF, which agrees with the FEA simulation. In addition, the RF field strength decreases as the distance from the microstrip resonator increases. The measurement shows that the expected deflection decreased as the distance from the microstrip resonator increased. Thus, the probe is qualitatively sensitive to the field strength.

Further RF measurements were performed and are reported elsewhere. Additional field measurement data are included in [15].

Authorized licensed use limited to: IEEE Xplore. Downloaded on November 24, 2008 at 14:41 from IEEE Xplore. Restrictions apply.

VI. Conclusion

In summary, we developed a process for the design of dielectric asymmetric trilayer cantilevers for calorimetric high-frequency near-field imaging. Kirchhoff's plate theory was used to estimate the curvature of the cantilevers due to thermal mismatch strain and residual stress developed during deposition and processing. FEA simulations validated the analytical results and experimental measurements. The analysis and experiment showed that an asymmetrical trilayered (nitride–oxide–nitride) structure is a better approach for the cantilever probes than a bimorph structure because it reduces the curvature associated with the thermal misfit strain developed during high temperature deposition.

References

[1] Y. Gao and I. Wolff, "A new miniature magnetic field probe for measuring three-dimensional fields in planar high-frequency circuits," *IEEE Trans. Microwave Theory Tech.*, vol. 44, pp. 911–918, Jun. 1996.

[2] D. Smith, "Signal and noise measurement techniques using magnetic field probes," in *Proc. 1999 IEEE Int. Symp. IEEE Electromagn. Compat.* , Aug. 2–6, 1999, vol. 1, pp. 559–563.

[3] V. Agrawal, P. Neuzil, and D. W. van der Weide, "A microfabricated tip for simultaneous acquisition of sample topography and high-frequency magnetic field," *Appl. Phys. Lett.*, vol. 71, no. 16, pp. 2343–2345, Oct. 1997.

[4] A. Jander, J. Moreland, and P. Kabos, "All-dielectric micromachined calorimeter for high-resolution microwave power measurement," in *Proc. 15th IEEE Int. Conf. Microelectromech. Syst. Conf.*, Jan 20–24, 2002, pp. 635–640.

[5] J. R. Barnes, R. J. Stephenson, C. N. Woodburn, S. J. O'Shea, M. E. Welland, T. Rayment, J. K. Gimzewski, and C. Gerber, "A femtojoule calorimeter using micromechanical sensors," *Rev. Sci. Instrum.*, vol. 65, no. 12, pp. 3793–3796, 1994.

[6] J. Moreland, M. Lohndorf, and P. Kabos, "Ferromagnetic resonance spectroscopy with a micromechanical calorimeter sensor," *Rev. Sci. Instrum.*, vol. 71, no. 8, pp. 3099–3103, 2000.

[7] J. Lai, T. Perazzo, Z. Shi, and A. Majumdar, "Optimization and performance of high resolution micro-optomechanical thermal sensors," *Sens. Actuators A, Phys.*, no. 58, pp. 113–119, 1997.

[8] L. B. Freund and S. Suresh, *Thin Film Materials: Stress, Defect Formation and Surface Evolution*. Cambridge, U.K.: Cambridge Univ. Press, 2003.

[9] Y. Zhang and M. Dunn, "Deformation of blanketed and patterned bilayer thin-film microstructures during post-release and cyclic thermal loading," *J. Microelectromech. Syst.*, vol. 12, no. 6, pp. 788–796, 2003.

[10] R. M. Jones, *Mechanics of Composite Materials*. Philadelphia, PA: Taylor & Francis, 1999.

[11] R. J. Wood, E. Steltz, and R. S. Fearing, "Optimal energy density piezoelectric bending actuators," *Sens. Actuators A, Phys.*, vol. 119, pp. 476–488, 2005.

[12] C. V. Thompson, "Structure evolution during processing of polycrystalline films," *Annu. Rev. Mater. Sci.*, vol. 30, pp. 159–190, 2000.

[13] P. J. French, P. M. Sarro, R. Mallee, E. J. M. Fakkeldij, and R. F. Wolffenbuttle, "Optimization of a low-stress silicon nitride process for surface-micromachining applications," *Sens. Actuators A, Phys.*, vol. 58, pp. 149–157, 1997.

[14] J. M. Olson, "Analysis of LPCVD process conditions for the deposition of low stress silicon nitride—Part 1: Preliminary LPCVD experiments," *Mater. Sci. Semiconduct. Process.*, vol. 5, pp. 51–60, 2002.

[15] S. Lee, T. M. Wallis, J. Moreland, Y. C. Lee, and P. Kabos, "Near-field imaging of high-frequency magnetic fields with calorimetric cantilever probes," *J. Appl. Phys.*, vol. 99, 2006.

Simone Lee received the B.S., M.S., and Ph.D. degrees in mechanical engineering from the University of Colorado at Boulder in 2003 and 2005, respectively.

From 2000 to 2003, she was a Research Assistant with the Department of Mechanical Engineering, University of Colorado at Boulder. She is currently with FormFactor, Inc., Livermore, CA, as a Principle Engineer in process development. She has authored and coauthored ten papers published in peer-reviewed conferences and journals.

Dr. Lee received a fellowship from the National Institute of Standards and Technology in the Professional Research Experience Program during 2003–2006. She received the Outstanding Ph.D. Dissertation Award in 2005 and the Academic Achievement Award in 2002 presented by the Department of Mechanical Engineering, University of Colorado at Boulder.

T. Mitch Wallis received the B.S. degree in physics from the Georgia Institute of Technology, Atlanta, in 1996 and the M.S. and Ph.D. degrees in physics from Cornell University, Ithaca, NY, in 2000 and 2003, respectively.

He holds a postdoctoral appointment at Colorado State University, Fort Collins. His research interests include the development of high-frequency scanning probe microscopes for the characterization of high-speed devices as well as high-speed nanoscale electronics.

Dr. Wallis received a National Research Council postdoctoral fellowship at the National Institute of Standards and Technology.

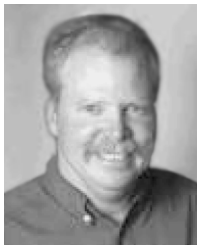

John Moreland received the B.S. degree in chemistry and physics from the University of Idaho, Boise, in 1977 and the Ph.D. degree in physics from the University of California, Santa Barbara, in 1984.

He joined the National Institute of Standards and Technology (NIST) in 1984, where he currently leads the Microsystems for Bio-Imaging and Metrology Project. The project designs, fabricates, and tests microelectromechanical systems for measurement applications in support of data storage, biotechnology, and telecommunications industries. Project members are taking a chip-scale microsystems approach in efforts to advance metrology instrumentation by improving sensitivity, portability, and cost as well as traceability to the International System of Units (SI).

Pavel Kabos (F'05) received the M.S. degree (with first class honors) in solid-state physics and the Ph.D. and habilitation (D.Sc.) degrees from Slovak University of Technology in 1970, 1979, and 1994, respectively.

He joined the Department of Electromagnetic Theory, Faculty of Electrical Engineering and Information Technology, as an Assistant in 1972 and became an Associate Professor in 1983. During 1982–1984, he was a Postdoctoral Fellow with the Department of Physics, Colorado State University, Fort Collins, where he returned in 1991 and as a Visiting Scientist, and later was a Research Professor, addressing the problems of linear and nonlinear high-frequency magnetism. In 1998, he joined the National Institute of Standards and Technology, Boulder, as a Visiting Scientist and became a Staff Physicist in the Electromagnetics Division in 2001. His research is on linear and nonlinear precession dynamics, metrology for high-speed electronics, magnetic force microscopy, dielectric and magnetic materials spectroscopy, nondestructive electromagnetic evaluation, and numerical methods for electromagnetic field analysis. He has authored or coauthored more than 90 archival papers on magnetics, several book chapters, and *Magnetostatic Waves and Their Applications* (New York: Chapman and Hall, 1994).

Authorized licensed use limited to: IEEE Xplore. Downloaded on November 24, 2008 at 14:41 from IEEE Xplore. Restrictions apply.

Y. C. Lee is a Professor of mechanical engineering at the University of Colorado, Boulder. He received the B.S.M.E. degree from National Taiwan University, Taiwan, R.O.C., in 1978 and the M.S. and Ph.D. degrees from the University of Minnesota, Minneapolis, in 1982 and 1984, respectively.

From 1993 to 2002, he was an Associate Director of the National Science Foundation (NSF) Center for Advanced Manufacturing and Packaging of Microwave, Optical and Digital Electronics, University of Colorado at Boulder. Prior to joining the university in 1989, he was a Member of Technical Staff with AT&T Bell Laboratories, Murray Hill, NJ. His research activities include packaging and thermal management of multichip modules, three-dimensional packaging, self-aligning soldering, fluxless or solderless flip-chip connections, optoelectronics packaging, process control using fuzzy-logic models, microelectromechanical systems (MEMS), molecular biology integrated with micro/nanoscale technologies, and atomic layer deposition for integrated micro/nanoelectromechanical systems (NEMS). He was an Associated Editor of *ASME Journal of Electronic Packaging* from 2001 to 2004

Dr. Lee is a Fellow of the American Society of Mechanical Engineers (ASME). He was a Guest Editor of IEEE TRANSACTIONS ON ADVANCED PACKAGING for two special issues on packaging of MEMS/NEMS in 2003 and 2005. He received the NSF Presidential Young Investigator Award in 1990.

Authorized licensed use limited to: IEEE Xplore. Downloaded on November 24, 2008 at 14:41 from IEEE Xplore. Restrictions apply.